AN INVESTIGATION OF THE AERODYNAMIC CHARACTERISTICS OF A COMBINED SWEPT BACK-SWEPT FORWARD WING CONFIGURATION

By

Luciano L. Mazzola and Eugene Mark Romer

Submitted in Partial Fulfillment of the Requirements
for the Degree of
Bachelor of Science in Aeronautical Engineering
at the
Massachusetts Institute of Technology

Signature of Authors Signature redacted ....
Signature redacted ....

Department of Aeronautical Engineering

May 25, 1953

Certified by Signature redacted ....
Thesis Supervisor

Cambridge, Massachusetts

May 25, 1953

Professor Earl B. Millard

Secretary of the Faculty

Massachusetts Institute of Technology

Cambridge, Massachusetts

Dear Sir:

In partial fulfillment of the requirement for the degree of Bachelor of Science in Aeronautical Engineering, we herewith submit our thesis entitled, "An investigation of the aerodynamic characteristics of a combined swept back-swept forward wing configuration."

Respectfully,

Signature redacted

Luciano L. Mazzola

Signature redacted

Eugene Mark Romer

ABSTRACT

AN INVESTIGATION OF THE AERODYNAMIC CHARACTERISTICS OF A COMBINED SWEPT BACK-SWEPT FORWARD WING CONFIGURATION

By

Luciano L. Mazzola
and
Eugene Mark Romer

Theoretical and experimental analysis of a combined swept back and swept forward wing configuration were made to determine the aerodynamic properties of the configuration.

The results showed fair correlation with existing airfoil data. Agreement between experimental and theoretical results indicated possible extension of the theory used to cover all possible variation of configuration. Results indicate that the configuration has possible practical applications.

ACKNOWLEDGEMENTS

The authors wish to extend their sincere appreciation and thanks to:

Professor Holt Ashley for his constant encouragement and guidance as thesis advisor.

Professor E.E. Larrabee for his invaluable help and guidance in regards to the test procedure and analysis of experimental data obtained from the wind-tunnel model.

Oscar Wallin and other members of the Aerolastic Shop for the assistance in the design and construction of the wind tunnel model.

George Fallon for his assistance and help in obtaining the photographs presented in this report.

Mrs. L.L. Mazzola for typing this report.

TABLE OF CONTENTS

Item		Page
Table of Illustrations		vi
List of Symbols		vii
Chapter I:	Introduction	1
Chapter II:	Theoretical Analysis and Calculations	
	2.1 Method of Attack	3
	2.2 Explanation of Equations and Use of Charts	3
	2.3 Theoretical Results	8
Chapter III:	Experimental Analysis and Calculations	
	3.1 Description of the Model	11
	3.2 Test Conditions	12
	3.3 Test Procedure	12
	3.4 Reduction and Correction of Data	13
	3.5 Experimental Results	13
Chapter IV:	Discussion	
	4.1 Correlation of Results	15
	4.2 Possible Arrangements of the Configuration in A Complete Airplane	15
	4.3 Suggestions for Future Investigation	16
References		17
Illustrations		18
Appendix		
	Table I Values of F Function	36
	Table II Coefficients of Circulations for Theoretical Calculations of Spanwise Load Distribution.	39
	Table III Coefficients of Circulations for Solution of Equation (2.14)	41

TABLE OF ILLUSTRATIONS

Fig.No.	Title	Page No.
1	Location of Lift and Downwash Points...............	18
2	Theoretical Spanwise Lift Distribution............	19
3	Three View Drawing of the Model...................	20
4	Top View of Model Before Fairing..................	21
5	Right Rear View of Model in Tunnel (with tufts)....	22
6	Rear View of Model in Tunnel (slight elevation)....	23
7	Front View of Model in Tunnel (with flaps down)....	24
8	Right Rear View of Model in Tunnel at a Negative Angle of Attack (with flaps down)................	25
9	Right Rear View of Model in Tunnel (with split elevators up)......................................	26
10	Tuft Study Diagrams...............................	27
11	Wind Tunnel Corrections...........................	30
12	Lift Coefficient vs. Angle of Attack--for Three Configurations......................................	31
13	Lift Coefficient vs. Moment Coefficient about aerodynamic Center--for three configurations..........	32
14	Lift Coefficient vs. Drag Coefficient--for three configurations..................................	33
15	Drag Coefficient vs. Lift Coefficient Squared for the Clean Condition................................	34

TABLE OF SYMBOLS

A	Aspect ratio
b	span (feet)
α	angle of attack
c	chord (1 foot)
C_L	coefficient of lift
C_D	coefficient of drag
C_{D_i}	coefficient of induced drag
C_m	pitching moment coefficient
F	downwash function
i	angle of incidence
K	local circulation
Γ	circulation distribution across wings
q	dynamic pressure slugs/feet sec^2
S	area of each wing (4.5 square feet)
S'	area of both wings (9 square feet)
s	semispan of horseshoe vortex
w	downwash (feet/sec)
V	stream velocity
X	distance from leading edge of center of wing aft, positive aft (in feet)
Y	distance from XY plane positive out along right wing in feet
Z	distance above and below plane of wing wake positive upward in feet
Δx_v	dimensionless difference in x coordinates of lift and downwash stations ($\Delta X/s$)
Δy_v	dimensionless difference in y coordinates of lift and downwash stations ($\Delta Y/s$)
Δz_v	dimensionless difference in z doordinates of lift and downwash stations ($\Delta Z/s$)

Chapter I

INTRODUCTION

The development of jet and rocket powered aircraft have resulted in aircraft structures designed explicitly for trans- and supersonic flight, such as the development of wing planforms with large angles of sweep-back or sweep-forward.

The use of swept-back planforms has posed problems not usually encountered in the aerodynamics of conventional planforms. One of the more serious of these is the problem of stalling at the wing tips at high angles of attack (such as in "flare out" landing conditions) thus rendering ailerons ineffective in preventing one wing or the other from dropping to the point where crashing is imminent.

Aircraft with swept-forward planforms do not have this difficulty, the stall pattern being such that stalling begins at the wing roots and progresses outboard. Full aileron control is maintained while landing and the danger of crashing because of uncontrollable rolling is eliminated. The disadvantage of this type of planform is that it is limited as to the speed at which it can fly safely since it reaches a speed in the upper sub-sonic range where the aerodynamic twisting moment exactly equals the structural restoring moment. At this point, a small gust is enough to cause the wings to twist off.

It was the authors' idea to combine the two wing shapes in order to determine if possibly the use of both types of planforms would eliminate the disadvantages of both and would combine the advantages inherent in both designs.

Chapter II

THEORETICAL ANALYSIS AND CALCULATIONS

2.1 METHOD OF ATTACK

In order to obtain the theoretical spanwise lift distribution across the wings, it was necessary to ascertain (1) the manner in which the airflow across a wing varied and (2) how this flow was influenced by the presence of another wing located in the flow field of the first. This means that the downwash at any point was the sum of the effect of the wing itself and the interference effect of the other wing.

2.2 EXPLANATION OF EQUATION AND USE OF CHARTS

The downwash angle at any point $P(x+\Delta x,\ y+\Delta y,\ z+\Delta z)$ due to a horseshoe vortex of semispan S located at a point Q(x,y,z) may be found from the relation

$$\frac{w}{V}(\Delta X, \Delta Y, \Delta Z) = \frac{K}{4\pi V s} F(\Delta X_v, \Delta Y_v, \Delta Z_v) \qquad (2.1)$$

(Ref. 1), where the function F is a function of the geometry of the wing and the coordinates of the lift and downwash points.

The function $F(\Delta X_v, \Delta Y_v, \Delta Z_v)$ may be found from the relationship

$$F = -\frac{2}{\Delta Y_v^2 - 1} \; \frac{1 - \dfrac{\Delta Z_v^2}{\Delta Y_v^2 - 1}}{\left(1 - \dfrac{\Delta Z_v^2}{\Delta Y_v^2 - 1}\right)^2 + 4\,\dfrac{\Delta Y_v^2\,\Delta Z_v^2}{(\Delta Y_v^2 - 1)^2}}$$

$$+\frac{\Delta X_v}{\Delta X_v^2+\Delta Z_v^2}\left\{\frac{1+\dfrac{\Delta X_v^2+\Delta Z_v^2}{\Delta Z_v^2+(\Delta Y_v+1)^2}}{\sqrt{\dfrac{\Delta X_v^2+\Delta Z_v^2}{(\Delta Y_v+1)^2}+1}}-\frac{1+\dfrac{\Delta X_v^2+\Delta Z_v^2}{\Delta Z_v^2+(\Delta Y_v-1)^2}}{\sqrt{\dfrac{\Delta X_v^2+\Delta Z_v^2}{(\Delta Y_v-1)^2}+1}}\right\} \qquad (2.2)$$

from reference 5.

For the special case $\Delta Z_v = 0$,

$$F = -\frac{2}{\Delta Y_v^2-1} \mp \frac{1}{\Delta X_v}\left[\sqrt{1+\left(\frac{\Delta X_v}{\Delta Y_v-1}\right)^2}-\sqrt{1+\left(\frac{\Delta X_v}{\Delta Y_v+1}\right)^2}\right] \qquad (2.3)$$

where the minus sign applies for positive values of ΔY_v and plus sign, for negative values.

The following special cases are also of interest

$$F(\Delta X_v, 0, \Delta Z_v) = \frac{2}{\Delta Z_v^2+1}+\frac{2\,\Delta X_v}{\Delta X_v^2+\Delta Z_v^2}\left\{\frac{1+\dfrac{\Delta X_v^2+\Delta Z_v^2}{\Delta Z_v^2+1}}{\sqrt{\Delta X_v^2+\Delta Z_v^2+1}}\right\} \qquad (2.4)$$

$$F(\Delta X_v, 0, 0) = 2\left(1+\frac{1}{\Delta X_v}\sqrt{1+\Delta X_v^2}\right) \qquad (2.5)$$

For the configuration under investigation nine horseshoe vortices of semispan 0.25' were assumed across each of the two wings. The centers or "lift" point of each vortex was located on the quarter-chord line of each wing positioned at stations located at 0, 22.2, 44.4, 66.6, and 88.8% of the wing semispan from the wing roots.

Stations one through nine inclusive refer to the downwash and lift points on the forward wing. Stations ten through eighteen correspond to the lift and downwash points on the rear wing.

The downwash points were chosen on the three-quarter chord line of the wings and at the same distances from the wing roots as the lift points. (see fig. 1)

The values of the F function in the plane of the wings were obtained from the charts provided with reference 2. The values of this function for coordinates located out of the plane of the wings were obtained by interpolation in the tables of reference 2 for the value of $\Delta Z_v = \pm 2$. Since. this table only allows direct interpolation of values of F for positive values of ΔX_v the following relation was used to obtain downwash values for negative values of ΔX_v

$$F(-\Delta X_v, \Delta Y_v, \Delta Z_v) = 2F(0, \Delta Y_v, \Delta Z_v) - F(\Delta X_v, \Delta Y_v, \Delta Z_v) \tag{2.6}$$

where the last two functions are easily obtained from the tables mentioned above.

Summing up all the contributions to the downwash due to the vortices we obtain

$$\alpha_m \equiv \left(\frac{\omega}{V}\right)_m = \frac{1}{4\pi V s} \sum_{n,m=1}^{n,m=18} F_{mn} K_n \tag{2.7}$$

where F_{mn} is the value of the F function at the downwash point "m" due to the dimensionless distances from the lift point "n".

For this particular case, s = .25, the symmetrical nature of the problem (i.e. $K_1 = K_9$, $K_2 = K_8$, ...; $K_{10} = K_{18}$, $K_{11} = K_{19}$,...;

$$\alpha_1 = \alpha_2 = \alpha_3 = \dots = \alpha_9 \; ; \; \alpha_{10} = \alpha_{11} = \alpha_{12} = \dots = \alpha_{18} \,)$$

reduces the solution of the variables to a system of ten simultaneous equations in ten unknown circulations and the local angles of attack. The resulting equations are of the form

$$a_{10} K_1' + a_{11} K_2' + \dots + a_{14} K_5' + a_{15} K_{10}' + \dots + a_{19} K_{14}' = P_1 \qquad (2.8)$$

$$a_{20} K_1' + a_{21} K_2' + \dots + a_{24} K_5' + a_{25} K_{10}' + \dots + a_{29} K_{14}' = P_2$$

etc.

where P_1, P_2, etc. are the local angles of attack; K_1', K_2', etc. are the values of the circulations K_1, K_2,... each multiplied by the factor $(\frac{1}{\pi V})$; and a_{10}, a_{11}, a_{12},...are the values obtained by adding the F functions of equivalent circulations together (i.e., combining the coefficients of K_1 & K_9, K_2 & K_8, etc.)

The solution of these equations is accomplished by setting the values of P_1 through P_5 equal to one, while holding P_6 through P_{10} equal to zero, and then setting $P_6, \dots, P_{10}$ equal to one while holding $P_1, \dots, P_5$ equal to zero.

We finally obtain each of the circulations (K_1, K_2 ...) as functions of the angles of attack of the front and rear wings and we can set up a Fourier series of the form $\Gamma = \sum_{n=1}^{n} \Gamma_n \sin(n\theta)$ (2.9) to represent the distribution of the circulation across each wing.

The circulation across each wing was assumed to be of the form $\Gamma = \Gamma_1 \sin\theta + \Gamma_3 \sin 3\theta + \Gamma_5 \sin 5\theta + \Gamma_7 \sin 7\theta + \Gamma_9 \sin 9\theta$ (2.10) where θ is defined by

$$\theta = \cos^{-1}\left(\frac{-y}{b/2}\right) \quad ; -\frac{b}{2} \leq y \leq \frac{b}{2}$$

The values of Γ_1, Γ_3, Γ_5, etc. can be obtained from the solution of the simultaneous equations for each wing in terms of the known circulations at specific stations, e.g.

$$\begin{aligned}
\Gamma_a &= \Gamma_1 \sin\theta_a + \Gamma_3 \sin 3\theta_a + \Gamma_5 \sin 5\theta_a + \cdots \\
\Gamma_b &= \Gamma_1 \sin\theta_b + \Gamma_3 \sin 3\theta_b + \Gamma_5 \sin 5\theta_b + \cdots \\
&\vdots \\
\Gamma_e &= \Gamma_1 \sin\theta_e + \Gamma_3 \sin 3\theta_e + \Gamma_5 \sin 5\theta_e + \cdots
\end{aligned} \tag{2.11}$$

where Γ_a, Γ_b, ... Γ_e are the values of the circulation of the first five stations across each wing and

$$\theta_a = \cos^{-1}\left(\frac{-y_a}{b/2}\right); \quad \theta_b = \cos^{-1}\left(\frac{-y_b}{b/2}\right); \quad \ldots$$

etc.

Only five equations in five unknowns are needed for each wing due to the symmetry of the loadings. Similarly only the odd values of "n" were assumed in the Fourier series because of the symmetrical load distribution. The value of the lift coefficient (C_L) becomes

$$C_L = \frac{\pi^2 b}{2S} \Gamma_1 \tag{2.12}$$

The coefficient of induced drag becomes

$$C_{D_i} = \frac{C_L^2}{\pi A} \sum_{n=1}^{n} n \left(\frac{\Gamma_n}{\Gamma_1}\right)^2 \tag{2.13}$$

2.3 THEORETICAL RESULTS

Theoretical results for basic loading (i.e. angle of incidence of the rear wing with respect to the front wing is equal to zero) were as follows:

$$\Gamma_{\alpha_1} = \pi\alpha V[.773\sin\theta + .254\sin 3\theta + .163\sin 5\theta + .258\sin 7\theta + .186\sin 9\theta] \tag{2.14}$$

$$\Gamma_{\alpha_2} = \pi\alpha V[.441\sin\theta + .111\sin 3\theta + .135\sin 5\theta + .144\sin 7\theta + .121\sin 9\theta] \tag{2.15}$$

where Γ_{α_1}, in the basic spanwise distribution of the circulation across the swept-back wing and Γ_{α_2} is the basic spanwise distribution of the circulation across the swept-forward wing due to the angle of attack .

Equation (2.12) becomes

$$C_L = \frac{\pi^2 b}{2S}\left(\frac{\Gamma_{\alpha_{11}} + \Gamma_{\alpha_{21}}}{2}\right) \tag{2.16}$$

or

$$C_L = \frac{\pi^2}{4}\frac{A}{b}\left(\Gamma_{\alpha_{11}} + \Gamma_{\alpha_{21}}\right) \tag{2.16a}$$

where A = Aspect Ratio, α is in radians, and b is the span in feet.

Equation (2.16) becomes

$$C_L = 2.92\alpha \tag{2.17}$$

Equation (2.13) becomes

$$C_{D_i} = 0.0722 C_L^2 \tag{2.18}$$

The value of the lift curve slope obtained was .051/°. The lift of the rear wing was theoretically about 53% of the lift of the front wing.

The circulation across each wing due to the angle of incidence (i) of the rear wing with respect to the front wing are given by

$$\Gamma_{i_1} = \pi i V[.296\sin\theta + .020\sin 3\theta - .350\sin 5\theta - .355\sin 7\theta - .090\sin 9\theta] \tag{2.19}$$

$$\Gamma_{i_2} = \pi i V[.492\sin\theta - .008\sin 3\theta + .014\sin 5\theta + .152\sin 7\theta + .178\sin 9\theta] \tag{2.20}$$

Combining equation (2.19) and (2.14) and (2.15) and (2.20) we get the circulation as functions of α and i.

$$\Gamma_{(\alpha+i)_1} = \pi V\Big[(.773\alpha+.296i)\sin\theta+(.254\alpha+.020i)\sin 3\theta+(.163\alpha-.350i)\sin 5\theta$$
$$+(.258\alpha-.355i)\sin 7\theta+(.186\alpha-.090i)\sin 9\theta\Big] \tag{2.21}$$

$$\Gamma_{(\alpha+i)_2} = \pi V\Big[(.411\alpha+.492i)\sin\theta+(.111\alpha-.008i)\sin 3\theta+(.135\alpha+.014i)\sin 5\theta$$
$$+(.144\alpha+.152i)\sin 7\theta+(.121\alpha+.178i)\sin 9\theta\Big] \tag{2.22}$$

We also obtain

$$C_L = \frac{\pi^2}{4}\frac{A}{b}\left(1.184\alpha+.788i\right) \tag{2.23}$$

In order to determine the angle of incidence at which the lift on both wings become equal the first coefficients of each circulation was equated. Equal lifts are obtained at values of $i = 1.85\alpha$. This means that at any given angle of incidence there is only one angle of attack at which the lift on both wings become equal. At this point

$$C_L = \frac{\pi^2 A}{4b}\Big[1.184+.788(1.85)\alpha\Big] \tag{2.24}$$

or

$$C_L = 6.5\,\alpha \tag{2.24a}$$

We also obtain for the induced drag

$$C_{D_i} = \frac{C_L^2}{2\pi A}\left\{2+3\left(\left[\frac{.234\alpha+.030i}{.773\alpha+.296i}\right]^2+\left[\frac{.111\alpha-.008i}{.411\alpha+.492i}\right]^2\right)\right.$$

$$\left.+5\left(\left[\frac{.163\alpha-.350i}{.773\alpha+.296i}\right]^2+\left[\frac{.135\alpha+.014i}{.411\alpha+.492i}\right]^2\right)\right.$$

$$+7\left(\left[\frac{.258\alpha-.355i}{.773\alpha+.296i}\right]^2+\left[\frac{.144\alpha+.152i}{.411\alpha+.492i}\right]^2\right)$$

$$+9\left(\left[\frac{.186\alpha-.090i}{.773\alpha+.296i}\right]^2+\left[\frac{.121\alpha+.178i}{.411\alpha+.492i}\right]^2\right)\Bigg\}$$

(2.25)

The value for C_{D_i} at $i = 1.85$ becomes (2.26)

$$C_{D_i} = 0.182\ C_L^2$$

Chapter III

EXPERIMENTAL ANALYSIS AND CALCULATIONS

3.1 DESCTIPTION OF THE MODEL

The model, consisting of two wings and supporting structure, is illustrated by a three-view drawing and several photographs comprising figures 3 thru 9.

The wings are constructed of laminated two inch pine strips. The wings have constant section NACA 0010 airfoils in the streamwise direction. Each wing has an area of 4.5 sq. ft., a one foot chord and a 4.5 foot span thereby giving each an aspect ratio of 4.5. Both wings have a taper ratio of one and no dihedral. The center lines of the wing chords are parallel and six inches apart. The ends of the wings are vertically above one another, lower wing being swept back 30° and the upper wing swept forward 30°.

The wings are held together by two 1/8 inch thick aluminum end plates and a 1/4 inch thick aluminum center strut. Wing tips were attached outboard of the end plates in order to eliminate sharp corners and thereby prevent airflow separation at the tips. The overall span of the model, including end plates and wing tips, is 55.75 inches.

The aluminum strips supporting the center butt joints of the wings, the angles supporting the center strut, and the holes in the front wings, which are necessary for supporting the model in the wind tunnel, can be seen in figure 4. All holes and exterior supports were faired in with modeling clay previous to the tests--as seen in figures 5 thru 9--in order to maintain a smooth flow of air over the model.

Two of the runs were made using partial span flaps extending from the center line of the wing to a point 26.75 inches outboard along the trailing edge (as seen in figures 5, 6 and 7). The flaps had a deflection of 40°, and a chord of 2.13 inches or 17.75% of the wing chord (both measured parallel to the air stream). In one run the flaps were attached to the upper side of the rear wing and in another run they were attached to the under side of the forward wing.

3.2 TEST CONDITIONS

The tests were conducted in the M.I.T. 4.5 x 6.0 foot wind tunnel at a pressure head of 4.385 inches of alcohol, which corresponds to an airspeed of 80 miles per hour. The test Reynolds number was 750,000 with a turbulence factor in the air stream of 2.7, based on spherical drag, which was caused by a turbulence net suspended across the tunnel, upstream of the model.

3.3 TEST PROCEDURE

Four runs were made in the tunnel, exclusive of those necessary for determining the tare and interference corrections. The lift, drag and pitching moment produced on three different configurations--namely clean, (figure 5 and 6), flaps down on forward wing (figure 7 and 8), elevator flaps up on rear wing (figure 9)--was measured while the angle of attack was taken from that at which a slightly negative lift was produced thru the stall point, by increments of 1 degree. One run was made with tufts on both wings in order to study the stall progression in the clean condition.

3.4 REDUCTION AND CORRECTION OF DATA

The following parameters were used in reducing the forces and moments obtained into coefficient form:

S' 9 square feet (total area of both wings)

c 1 foot (chord of one wing)

b 4.5 feet

q 16.37 slugs/feet sec^2

qS' 147.3 slugs feet/sec^2

qS'c 147.3 slugs $feet^2$/sec^2

The necessary corrections applied to the d ata are shown in figure 11. $\Delta\alpha_{ref}$ is a correction due to an incorrect setting of the angle of attack indicator. The $\Delta C_{m_{trans}}$'s were necessary to obtain the pitching moments about the aerodynamic centers from those about the trunnions. All other corrections are explained in reference 3, pages 124-132 andpage 225, equations (6:14) and (6:15). The tunnel wall interference factor, δ ,was found in reference 4, page 163.

3.5 EXPERIMENTAL RESULTS

The results of the tuft studies can be seen in figure 10, a,b, and c. For the sake of clarity the forward and aft wings have been separated in the drawings.

The corrected force and moment coefficients have been plotted as seen in figures 12,13,14,15.

From figure 10, it can be seen that the rear wing was still lifting at an angle of attack at which the front wing was completely stalled. This accounts for the leveling off of the lift curve after stall, as seen in figure 12. Severe buffiting of the rear wing, caused by the unsteady wake of the front wing flowing over it, was observed at high angles of attack.

In order to provide some means of comparison, calculations were made to obtain the amount of deflection of an equal span 20% chord sealed elevator needed to produce the moment obtained by the split elevator used on the model. Figures 2-58 and 9-15 of reference 5, were used for this purpose. The equivalent deflection was found to be 18.5°.

The aerodynamic centers were found to be at 76% of mac of the front wing clean condition, 88% of mac of the front wing with elevators up on the rear wing and, 73% of mac of the front wing with flaps down on the front wing.

As seen from figure 12, a maximun lift coefficient of .70 was obtained for the clean condition and .83 with flaps down, It can be observed from figure 13 that the pitching moment with flaps down at zero lift is + .18. It has been calculated (using figures 12 and 13) that the elevator deflection necessary to trim out this moment would cause an increase of C_L, at zero α , of .15 and an increase of the maximum lift of about .12 to a maximum C_L of about .90.

From figure 15, dC_D/dC_L^2 for the clean condition can be seen to be .145. Defining the Oswald efficiency factor "e" as ,
e is found to be .985.

Chapter IV

DISCUSSION

4.1 CORRELATION OF RESULTS.

Experimental and theoretical lift curve slopes of .056 and .051 agree fairly well, however, the polar lift-drag slopes of .145 and .072 do not agree. Possible reasons for lower theoretical values in these slopes are: 1) ignoring the effect of end plates in the theoretical calculations, 2) taking an insufficient number of downwash stations across the wings and, 3) possible experimental errors.

Both the theoretical and experimental results indicate a greater lift distribution on the forward wing for the configuration tested. Theoretical results indicate that higher lifts could be obtained by setting the rear wing at a positive angle of incidence with respect to the front wing.

4.2 POSSIBLE ARRANGEMENTS OF THE CONFIGURATION IN A COMPLETE AIRPLANE

The experimental tests show that with the chords of both wings parallel to each other the rear wing provides an excellent place to mount elevators. By mounting elevators on the inboard sections and ailerons on the outboard sections of the rear wing full span flaps could be then mounted on the front wing, whereas the tests have shown, they would be very effective.

Increasing the angle of incidence of the rear wing with respect to the forward wing could increase the lift on that wing to a value equal to that on the forward wing, as shown by the theoretical calculations, and thereby produce a diving moment about the aerodynamic center. This would then necessitate the addition of a tail behind the rear wing on which elevators would be mounted, while the two main wings would support some combination of ailerons and flaps.

4.3 SUGGESTIONS FOR FUTURE INVESTIGATION.

1) A more accurate theoretical analysis of the problem , taking into account the effects of end plates, angles of incidence of the rear wing and horigontal and vertical position of rear wing with respect to front wing.

2) An analysis of a dynamic model to determine flutter speed.

3) Possible design for a complete airplane using this wing configuration.

4) Response of Configuration to gust loading.

REFERENCES

1. Glauert, H.: The Elements of Aerofoil and Airscrew Theory. Cambridge University Press, 1926.
2. Diederich, Franklin W.: Charts and Tables for Use in Calculations of Downwash of Wings of Arbitrary Plan Form. N.A.C.A. T.N. 2353,1951.
3. Pope, Alan: Wind Tunnel Testing. John Wiley and Sons, Inc., New York 1947.
4. Bernbaum, Lawrence: Design Construction and Calibration of the M.I.T. 4.5 x 6.0 foot Wind Tunnel. M.I.T. S.M. Thesis, 1948.
5. Perkins, Courtland D. and Hage, Robert E.: Airplane Performance, Stability and Control. John Wiley and Sons Inc., New York 1950.
6. Purser, Paul E. and Spearman, M. Leroy: Wind-Tunnel Tests at Low Speed of Swept and Yawed Wings Having Various Plan Forms. N.A.C.A. T.N. 2445, 1951.

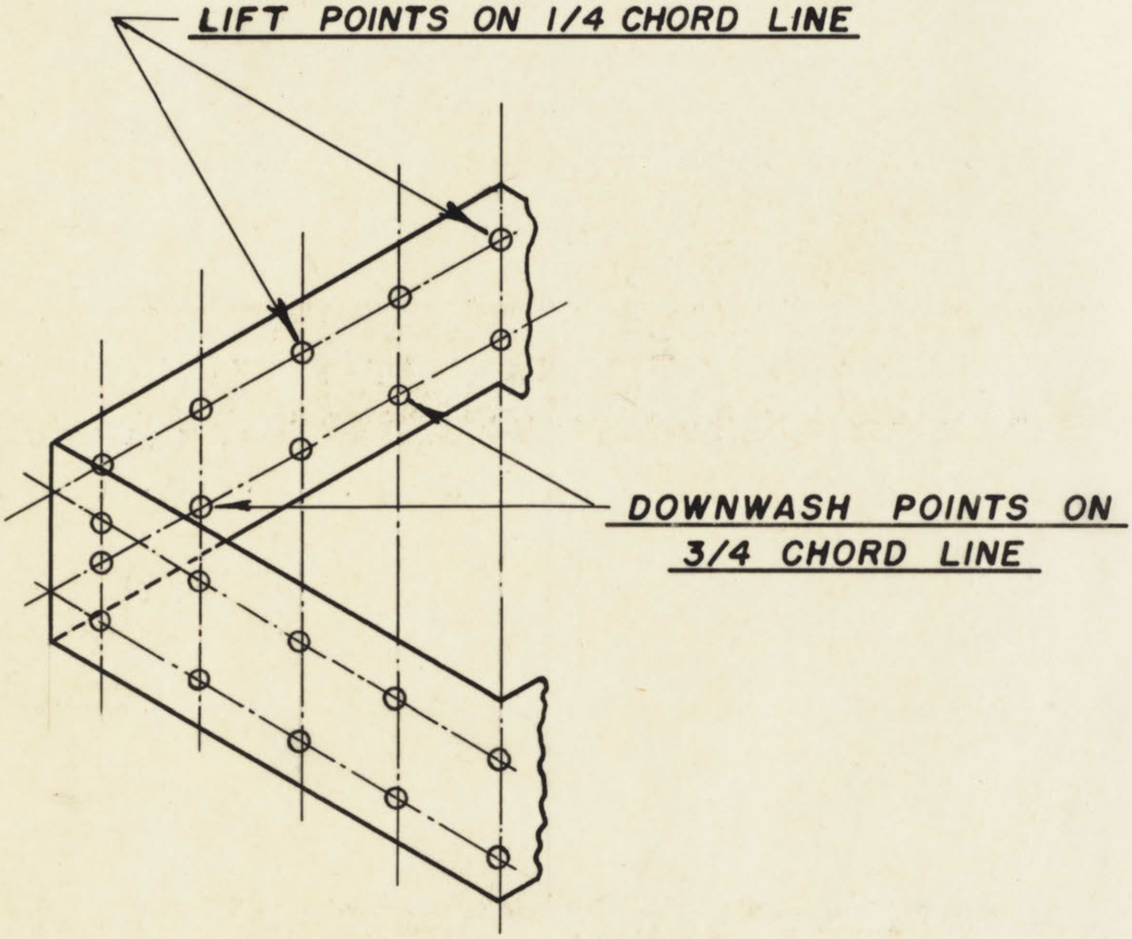

LOCATION OF LIFT AND DOWNWASH POINTS

figure 1

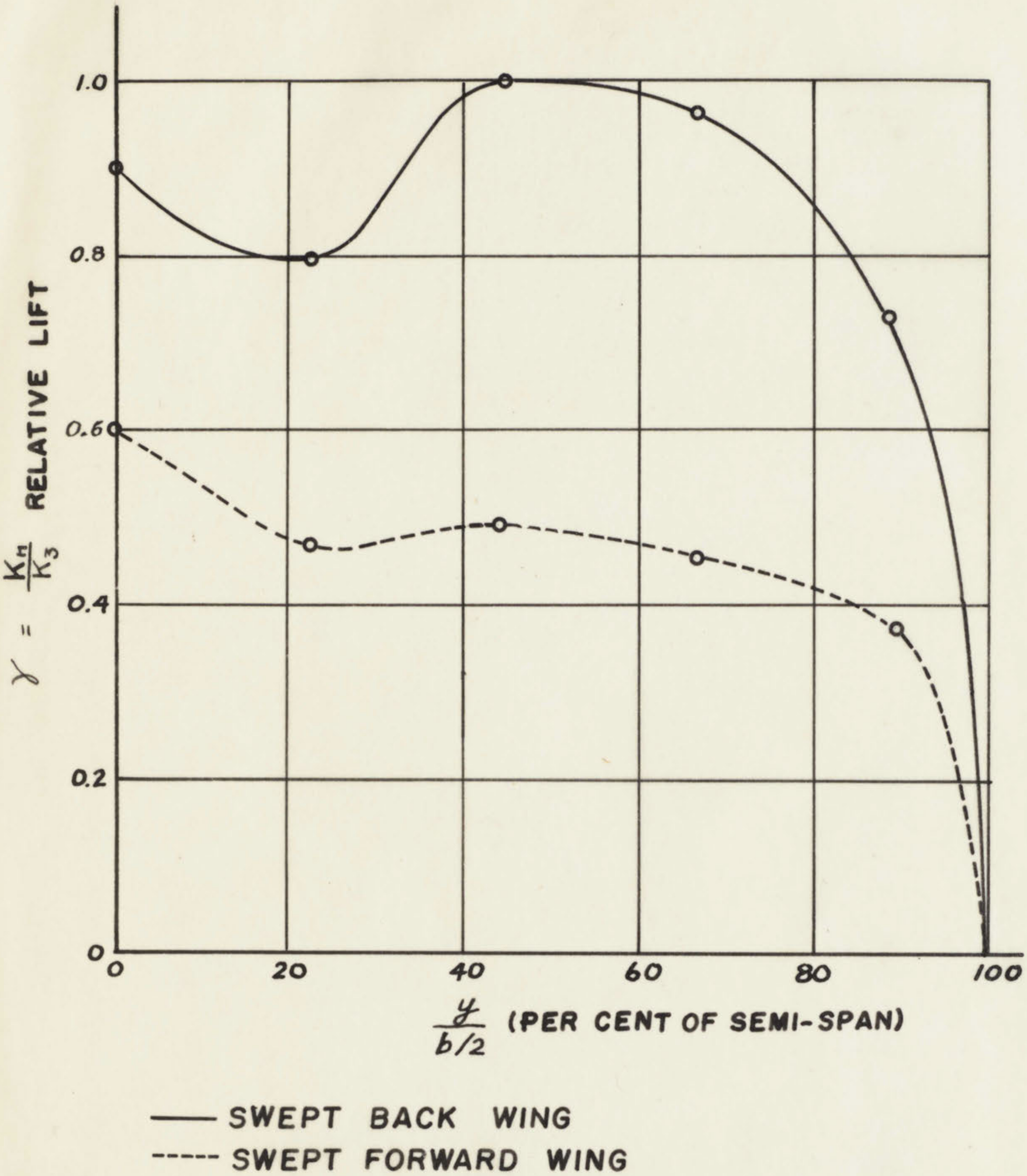

LIFT DISTRIBUTION VERSUS DISTANCE FROM

CENTER OF WINGS

fig. 2

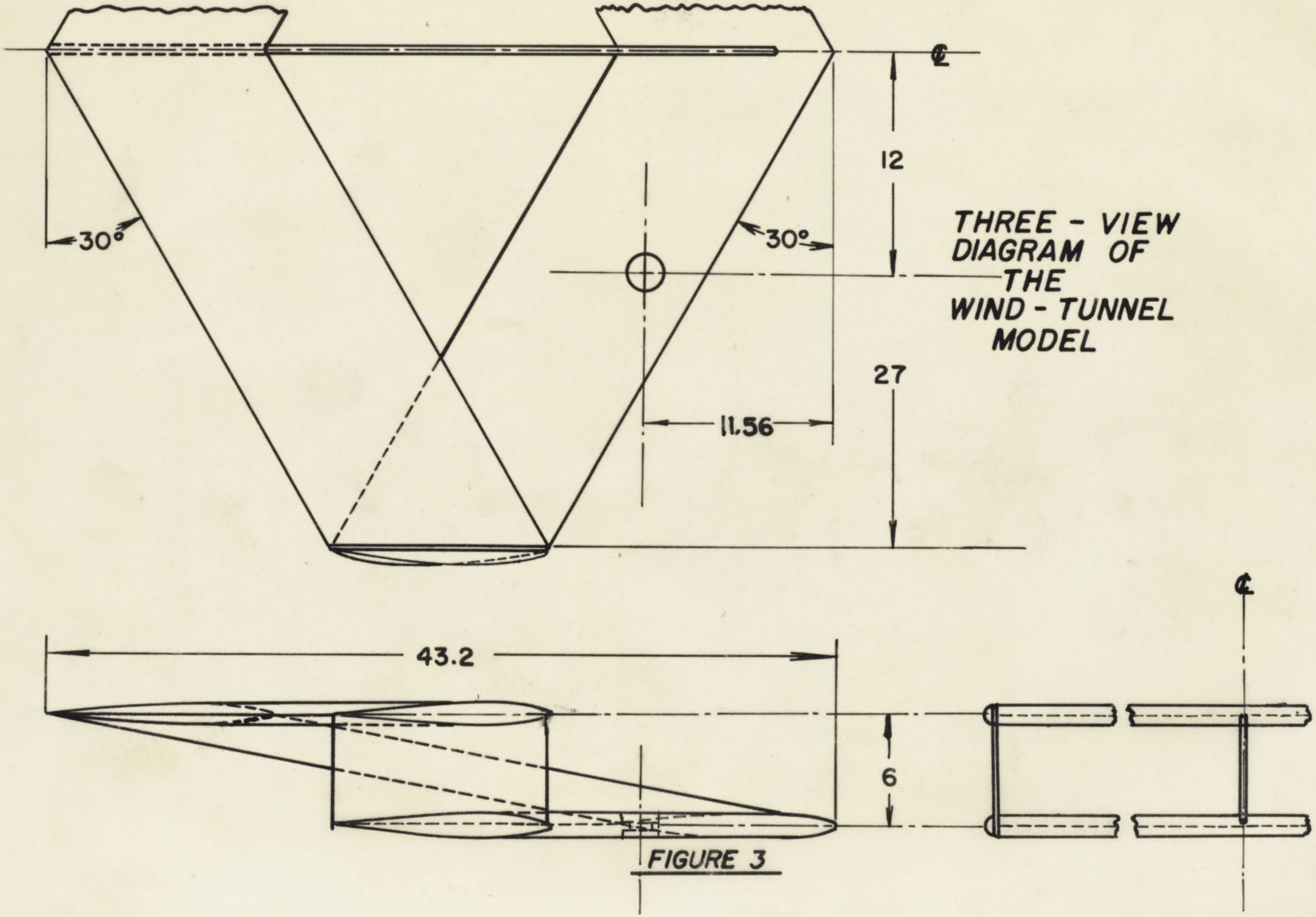

THREE - VIEW DIAGRAM OF THE WIND - TUNNEL MODEL

FIGURE 3

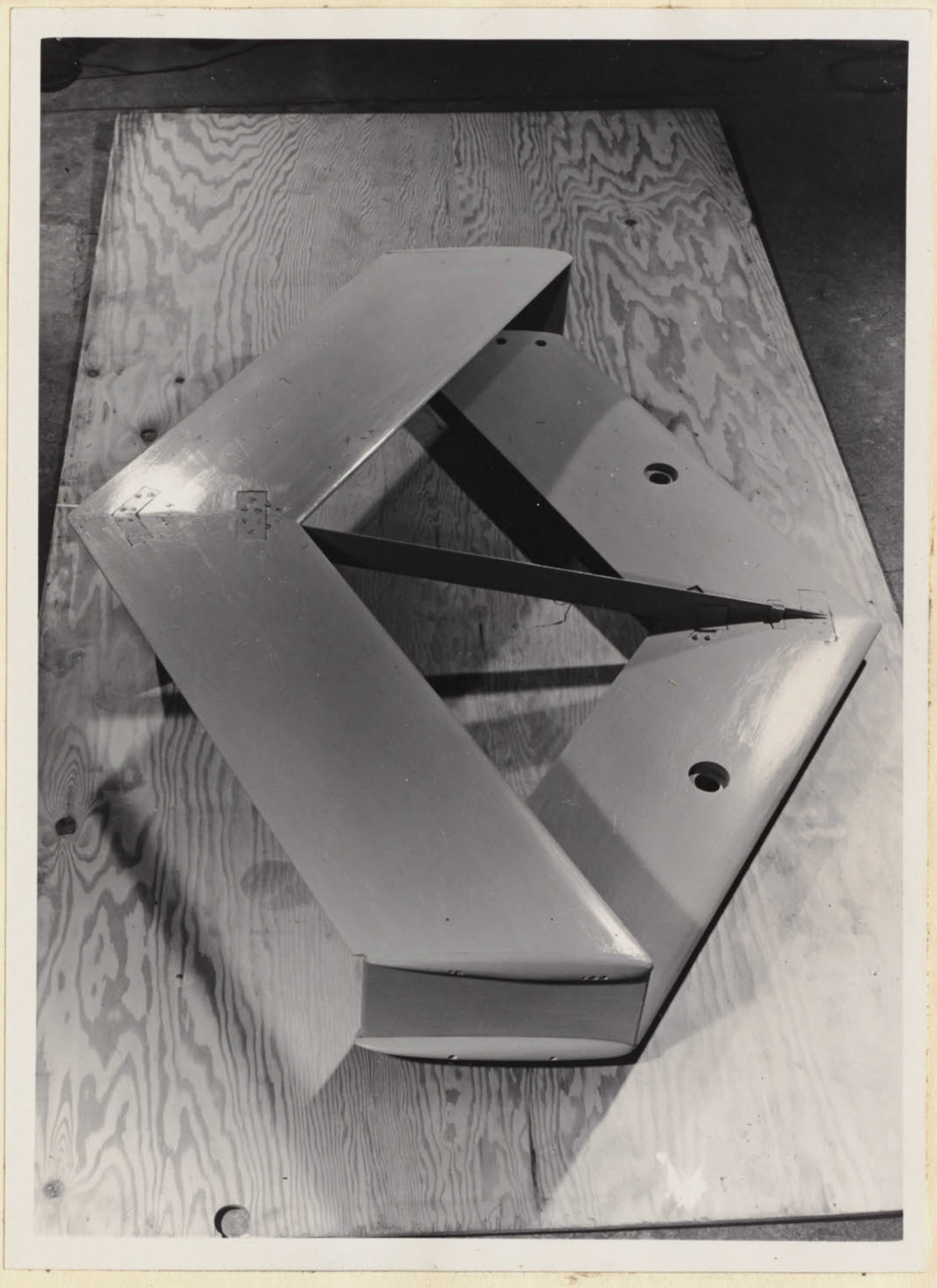

TOP VIEW OF MODEL BEFORE FAIRING (FIG. 4)

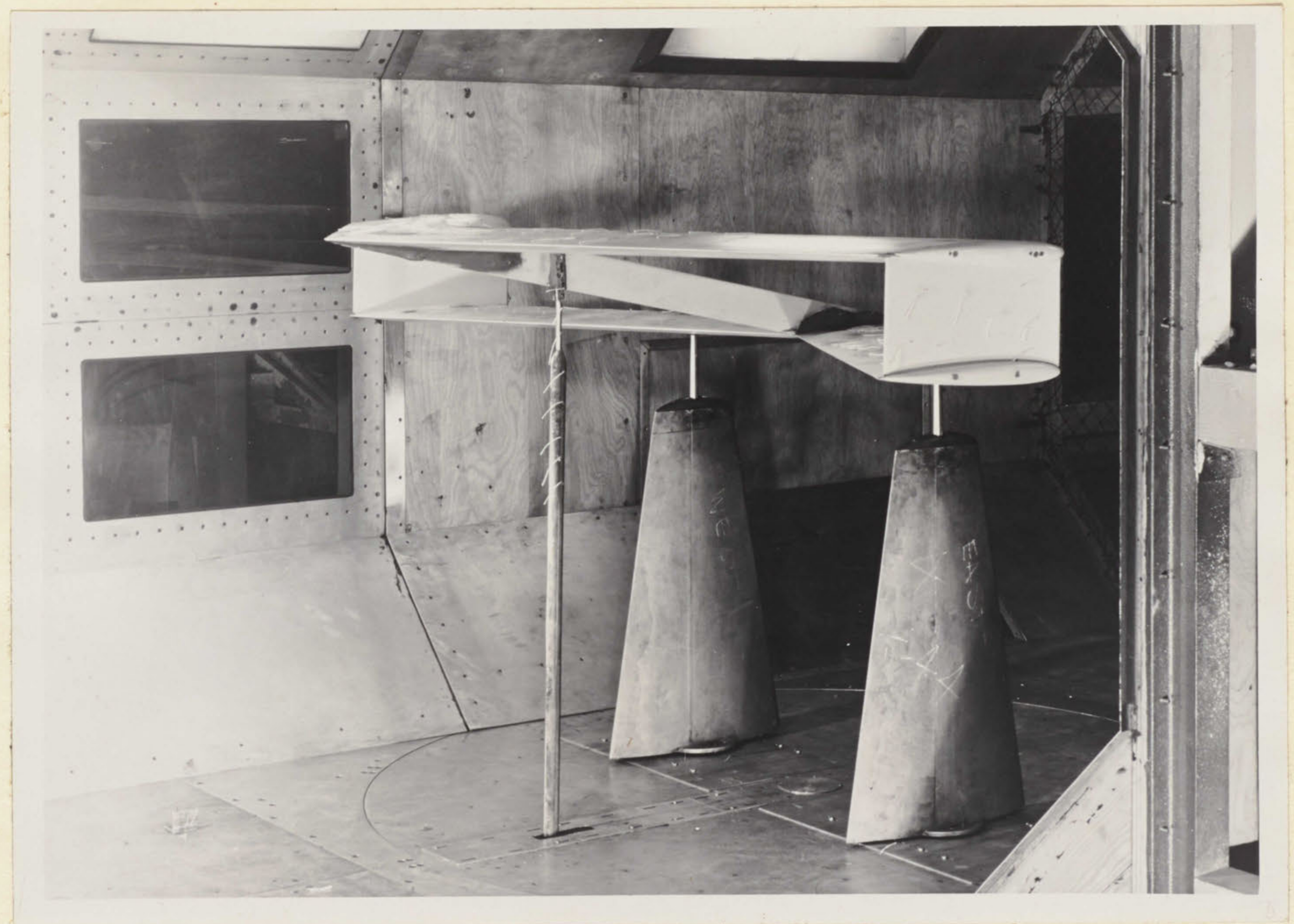

RIGHT REAR VIEW OF MODEL IN TUNNEL (WITH TUFTS) – FIGURE 5

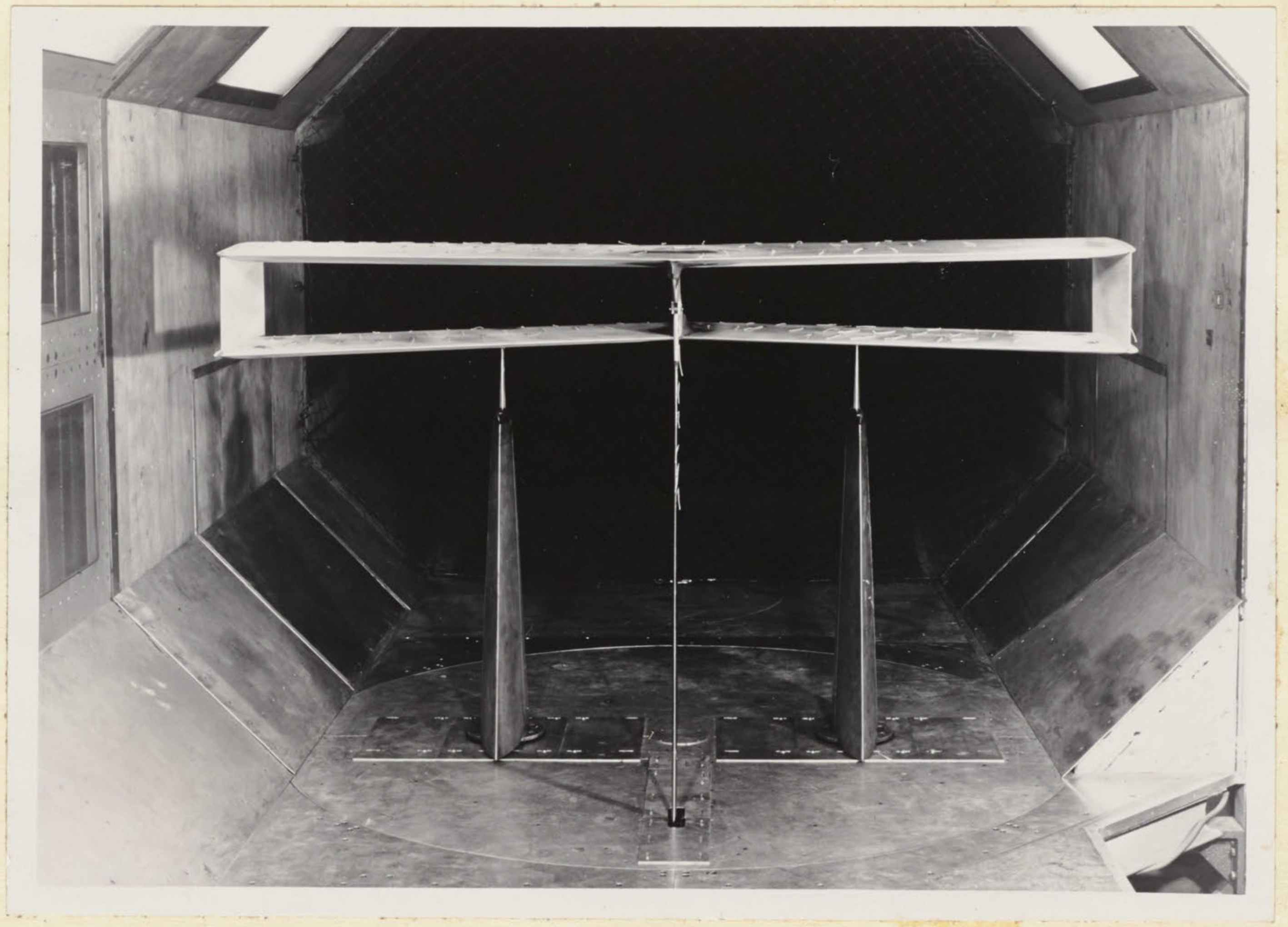

REAR VIEW OF MODEL IN TUNNEL (SLIGHT ELEVATION)

fig. 6.

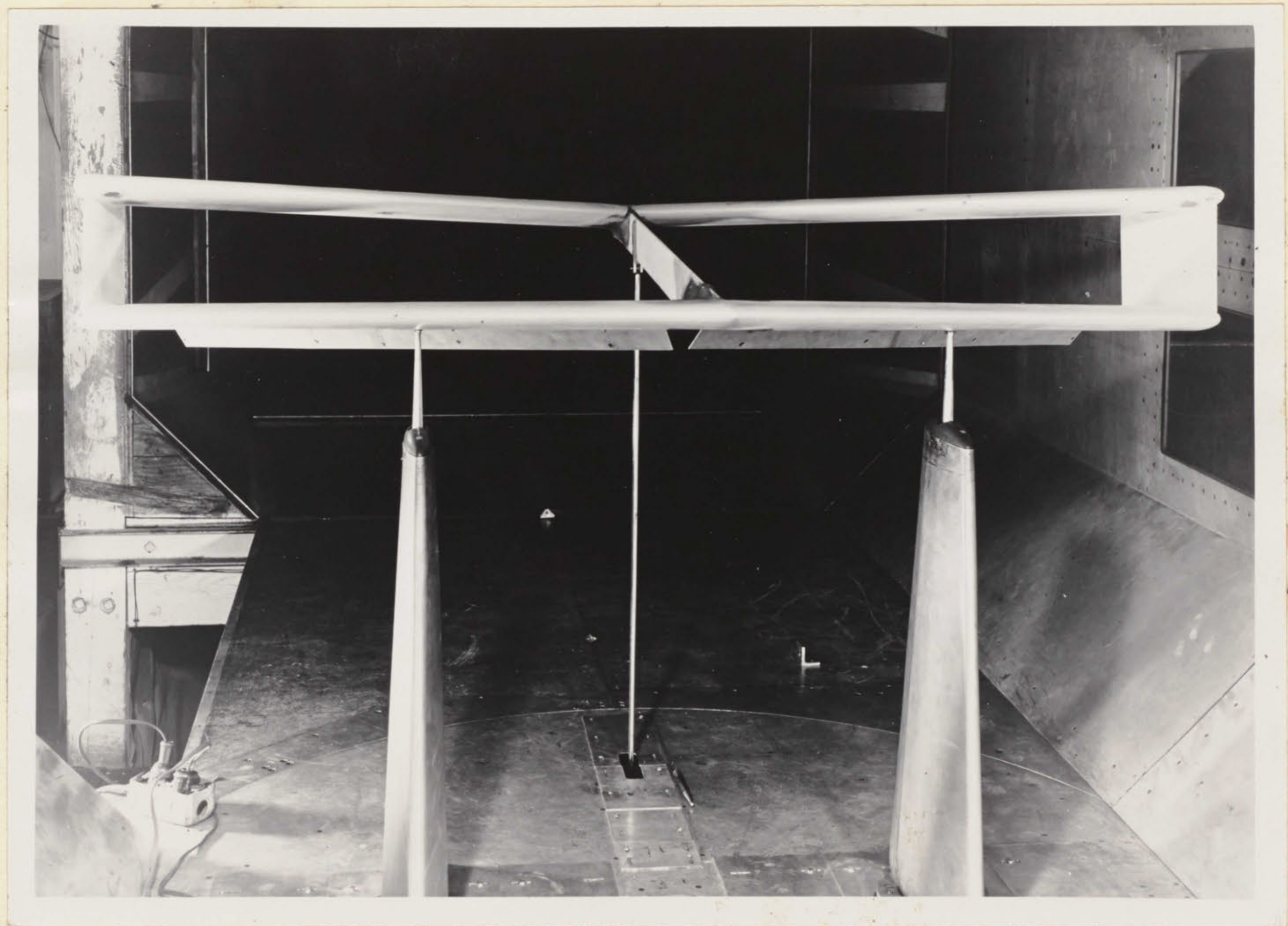

FRONT VIEW OF MODEL IN TUNNEL (FLAPS DOWN).

figure 7

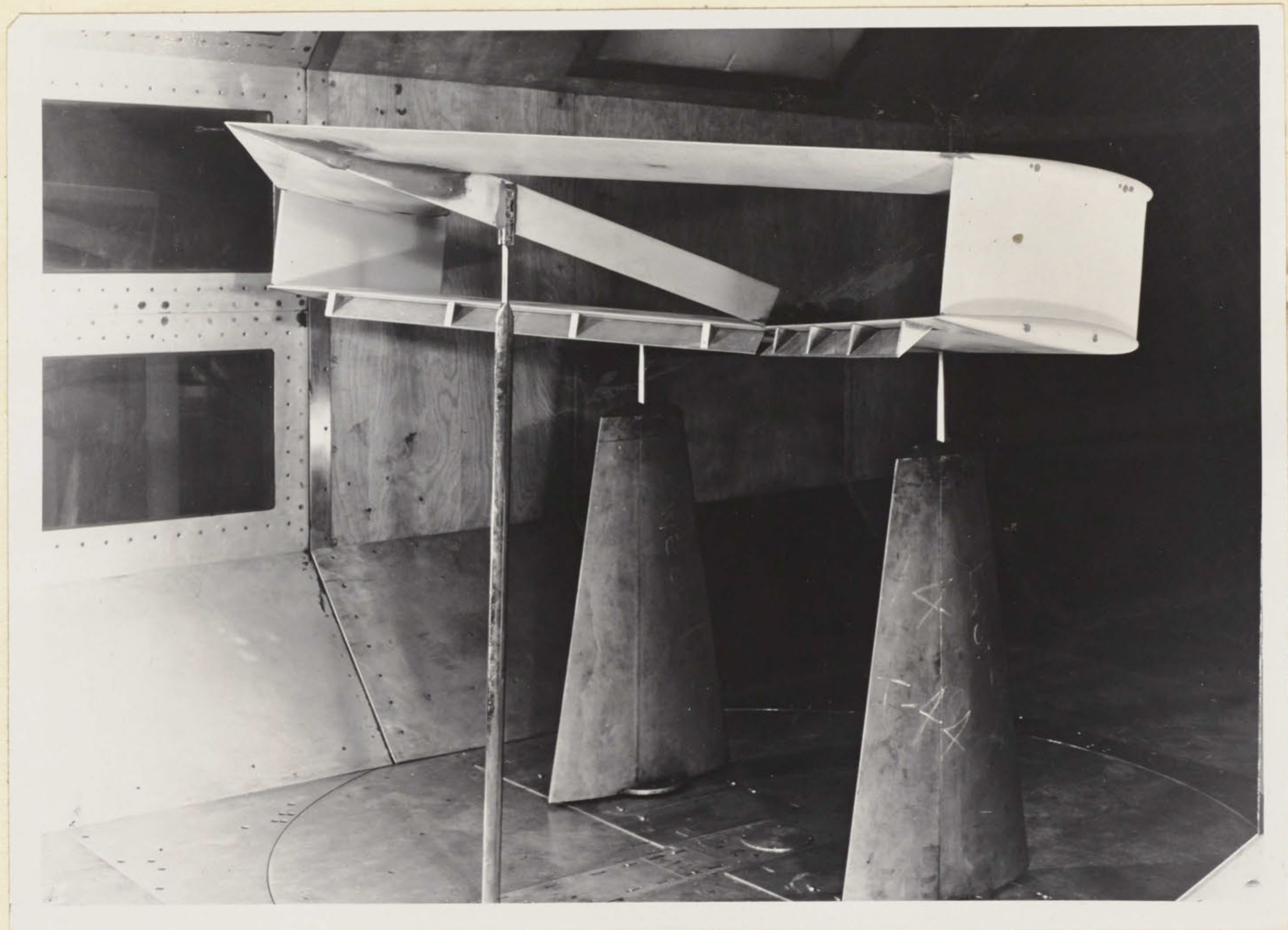

RIGHT REAR VIEW OF MODEL IN TUNNEL AT A NEGATIVE ANGLE OF ATTACK (FLAPS DOWN)

FIGURE 8

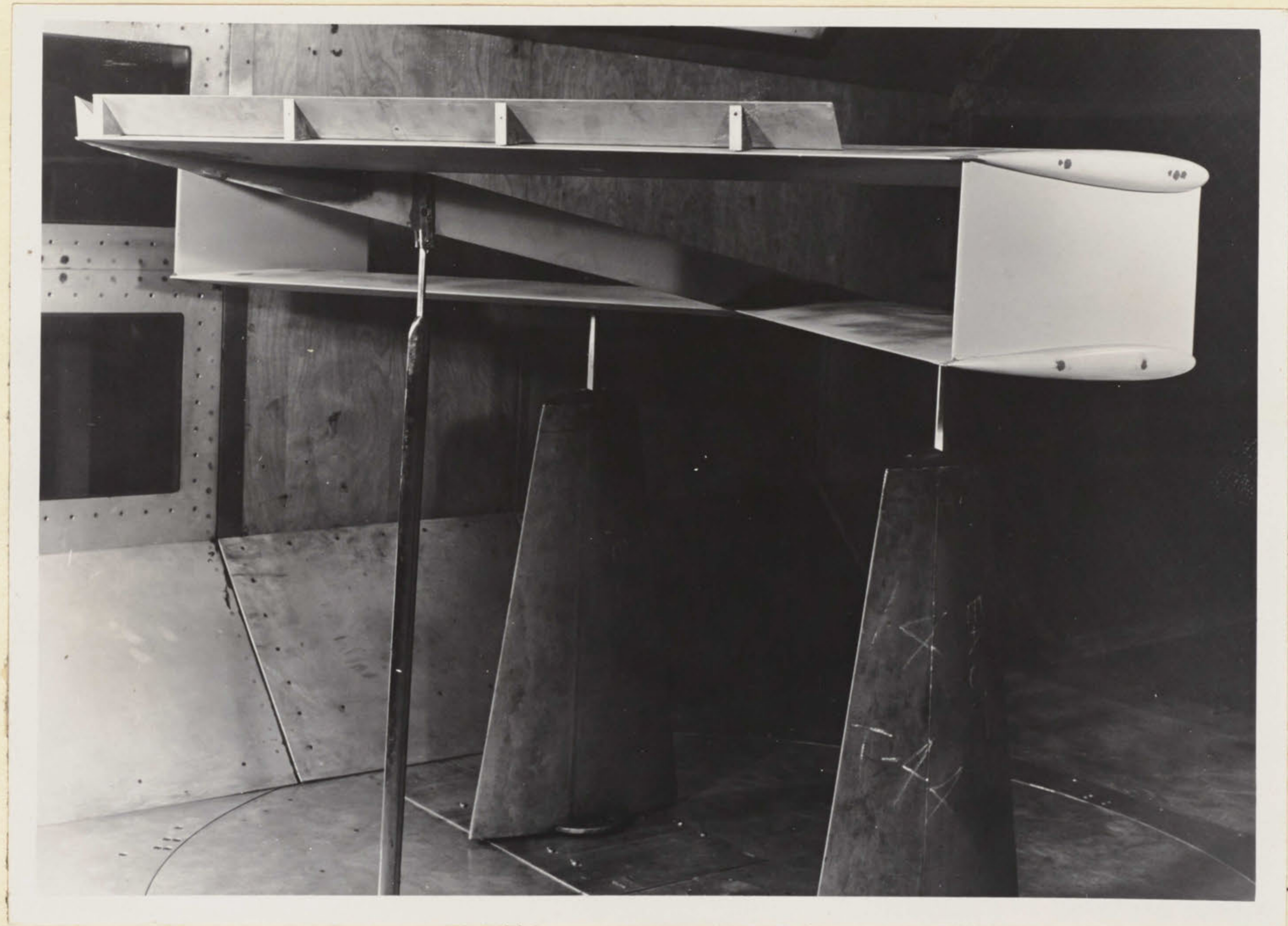

RIGHT REAR VIEW OF MODEL IN TUNNEL (SPLIT ELEVATORS UP)

FIGURE 9

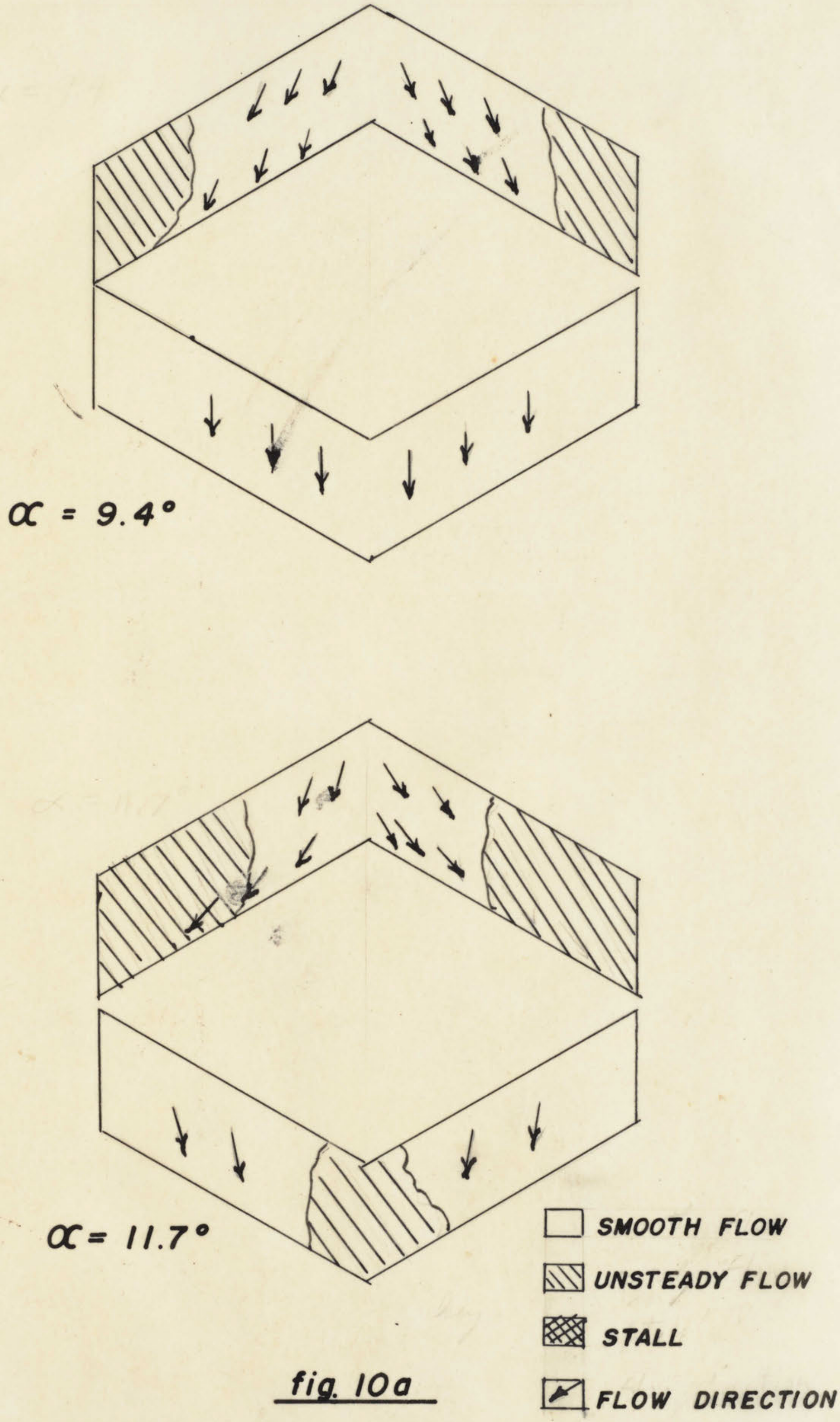

fig. 10a

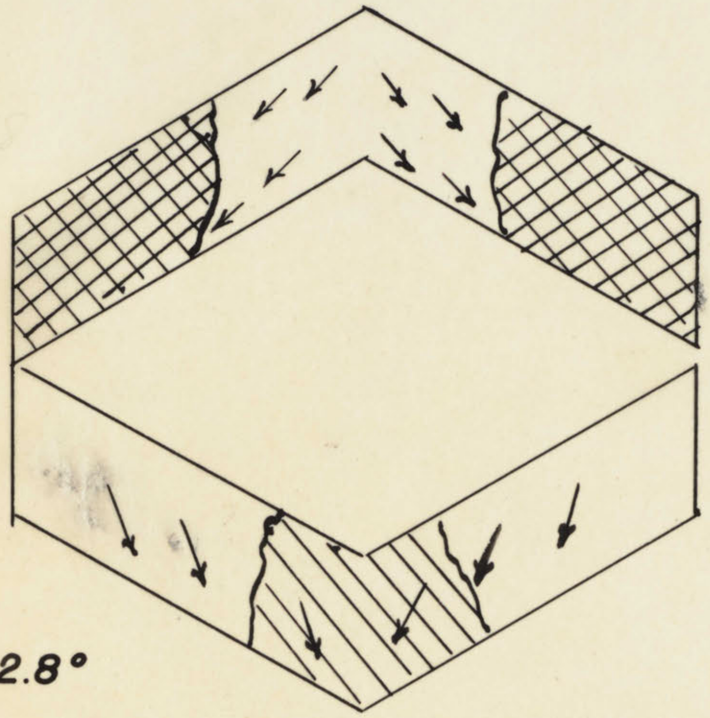

$\alpha = 12.8°$

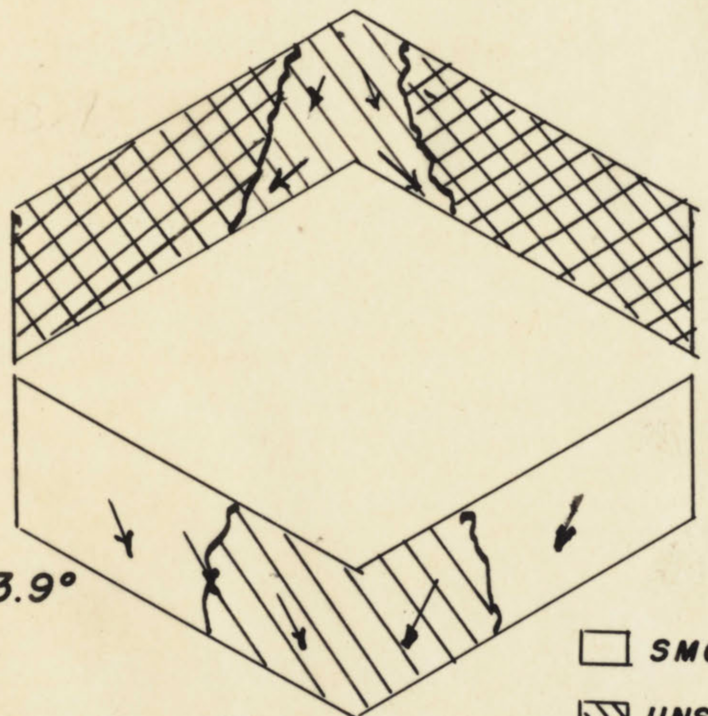

$\alpha = 13.9°$

SMOOTH FLOW

UNSTEADY FLOW

STALL

FLOW DIRECTION

fig. 10b

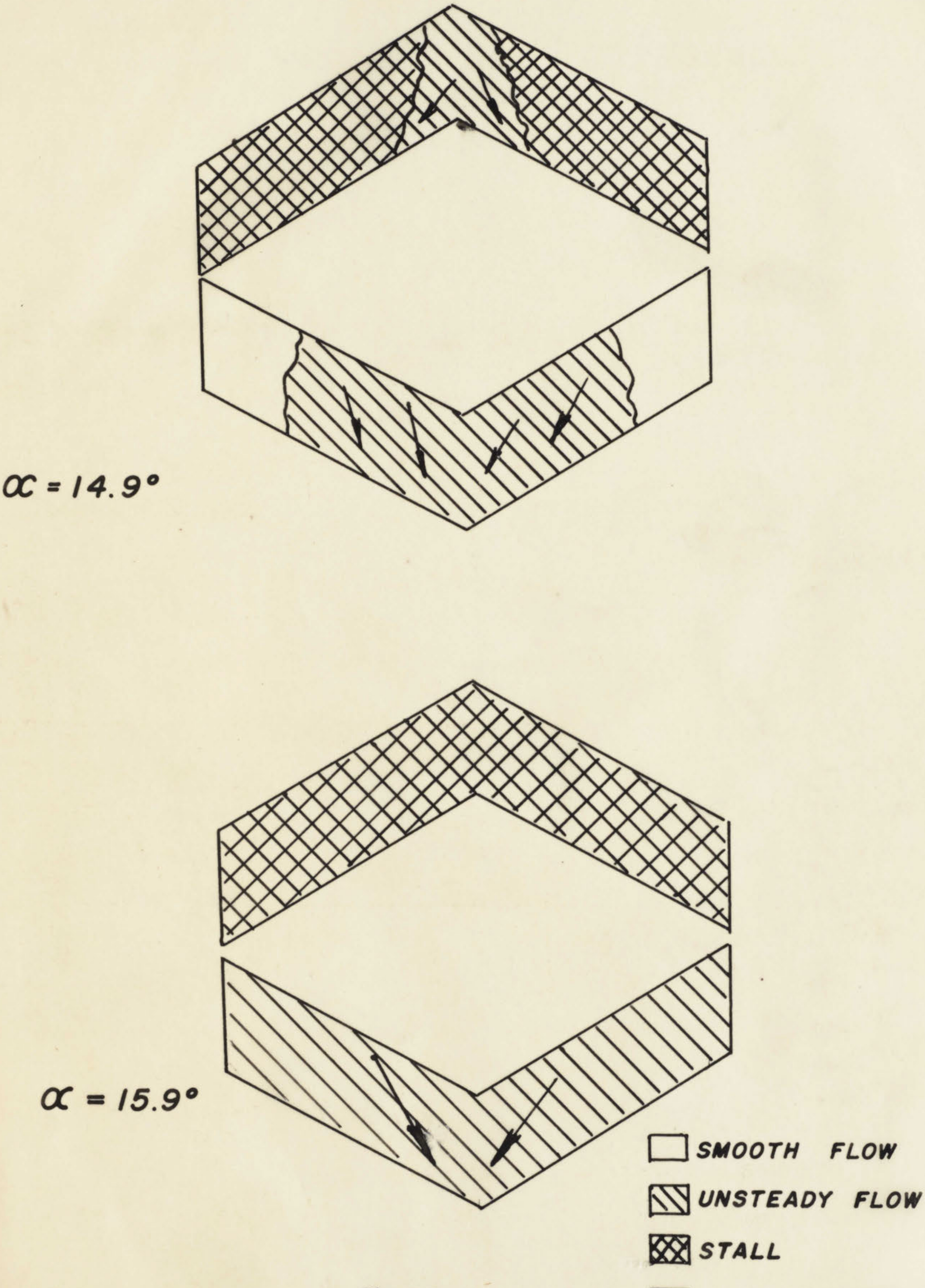

$\alpha = 14.9°$
$\alpha = 15.9°$
SMOOTH FLOW
UNSTEADY FLOW
STALL
FLOW DIRECTION

fig. 10c

WIND TUNNEL CORRECTIONS

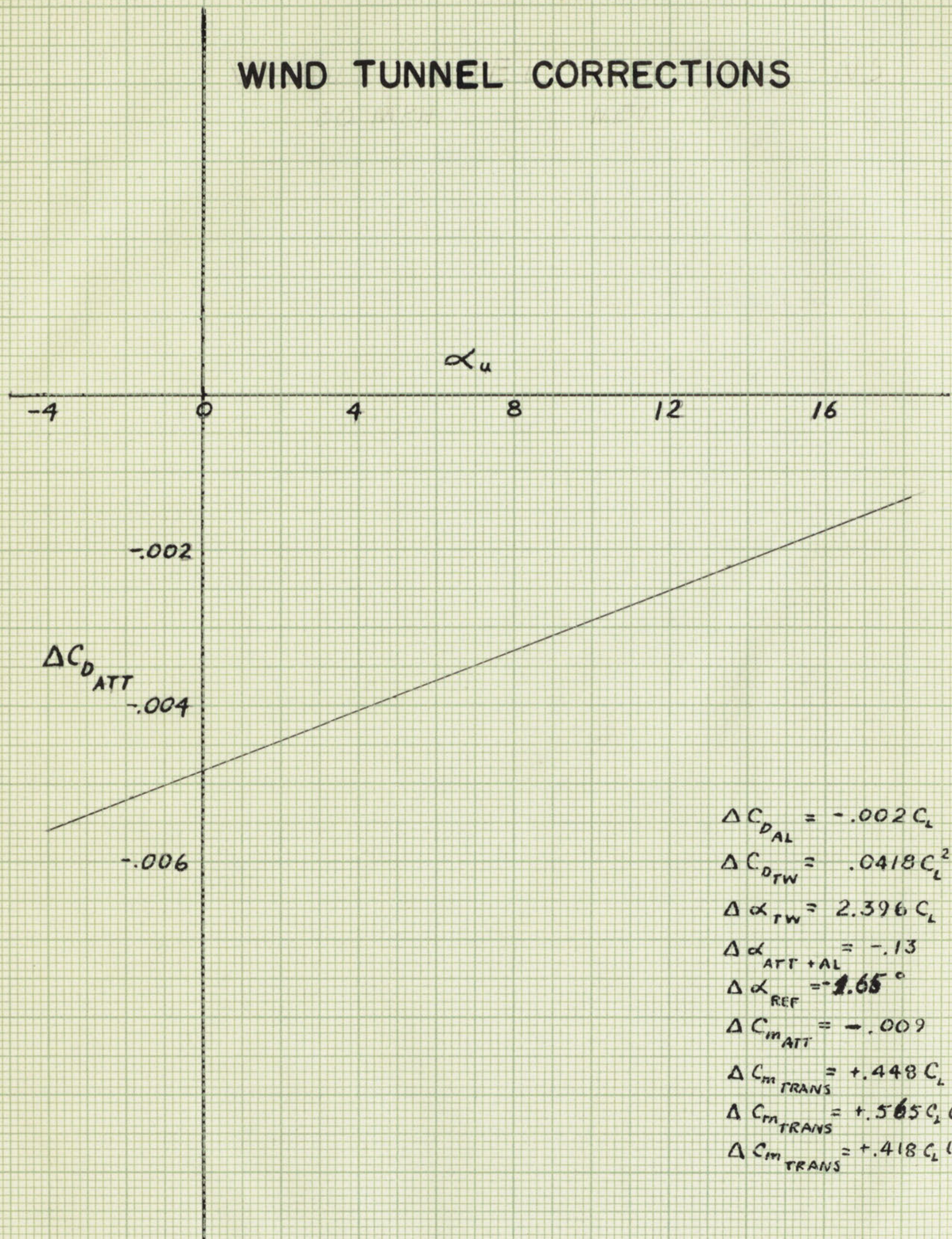

$\Delta C_{D_{AL}} = -.002\, C_L$

$\Delta C_{D_{TW}} = .0418\, C_L^2$

$\Delta \alpha_{TW} = 2.396\, C_L$

$\Delta \alpha_{ATT+AL} = -.13$

$\Delta \alpha_{REF} = -1.65^\circ$

$\Delta C_{m_{ATT}} = -.009$

$\Delta C_{m_{TRANS}} = +.448\, C_L$ (CLEAN)

$\Delta C_{m_{TRANS}} = +.565\, C_L$ (ELEVATORS)

$\Delta C_{m_{TRANS}} = +.418\, C_L$ (FLAPS)

fig. 11

LIFT COEFFICIENT VS. ANGLE OF ATTACK

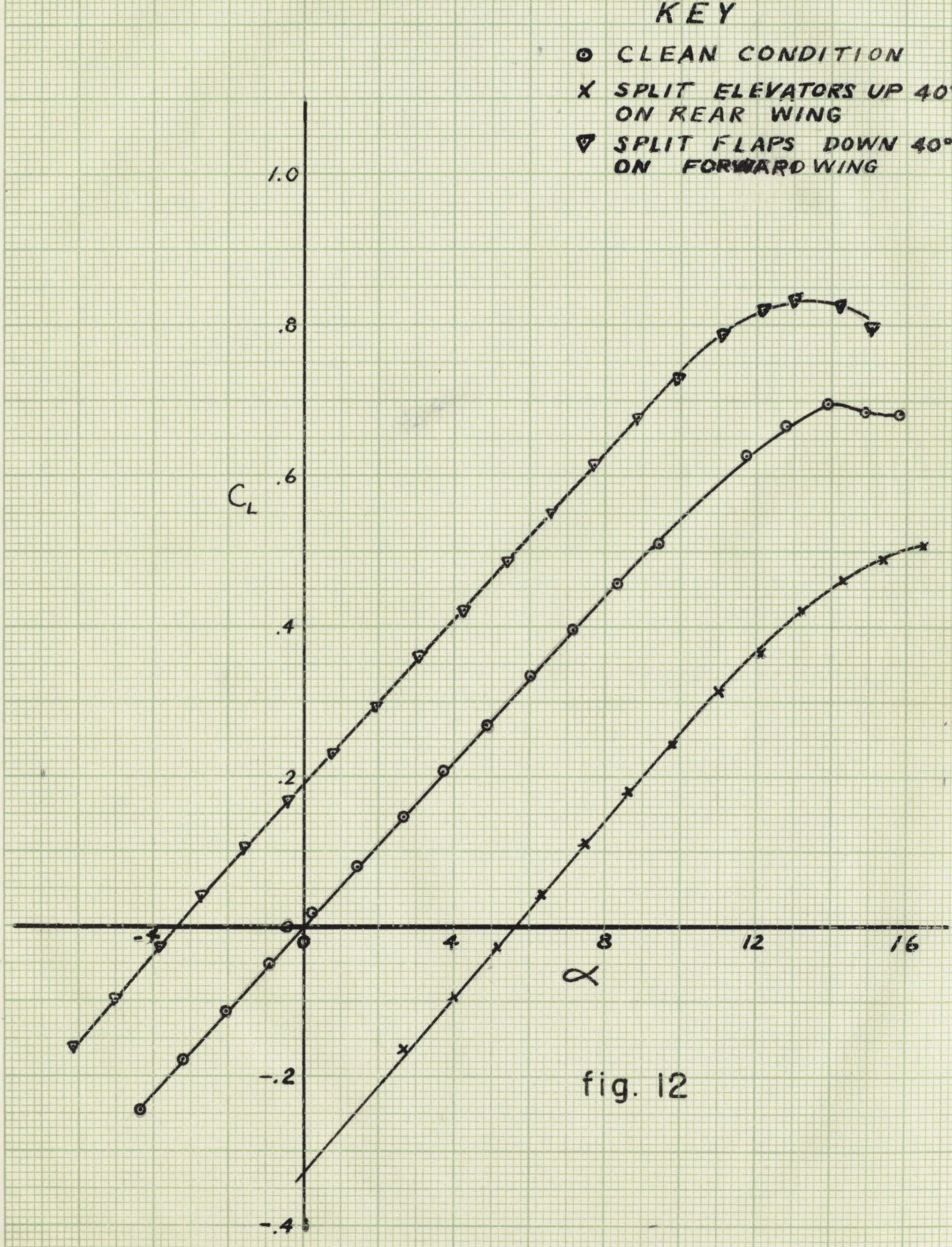

fig. 12

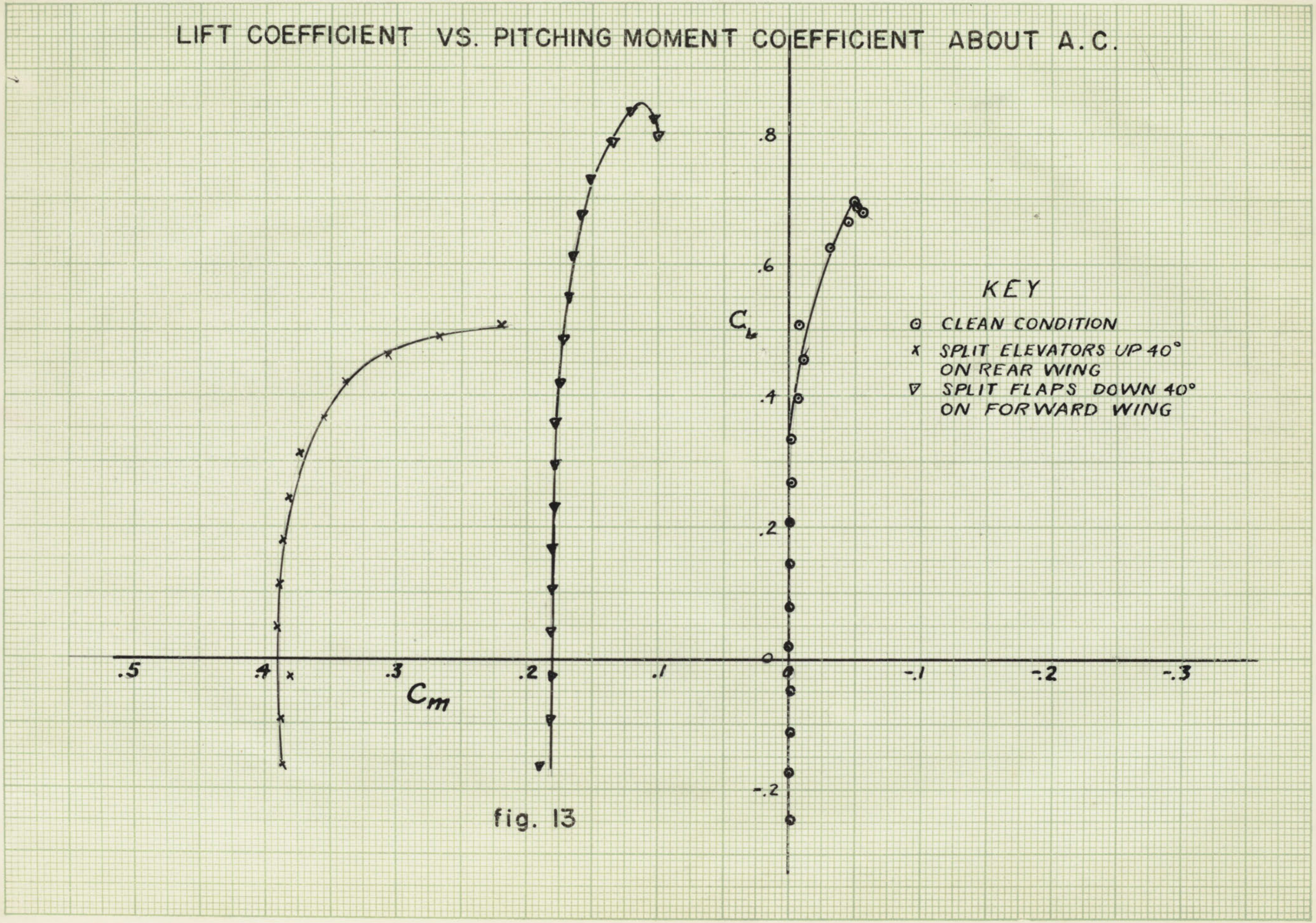
LIFT COEFFICIENT VS. PITCHING MOMENT COEFFICIENT ABOUT A.C.
KEY
CLEAN CONDITION
SPLIT ELEVATORS UP 40° ON REAR WING
SPLIT FLAPS DOWN 40° ON FORWARD WING
C_L
C_m
.8
.6
.4
.2
0
-.2
.5
.4
.3
.2
.1
-.1
-.2
-.3
fig. 13

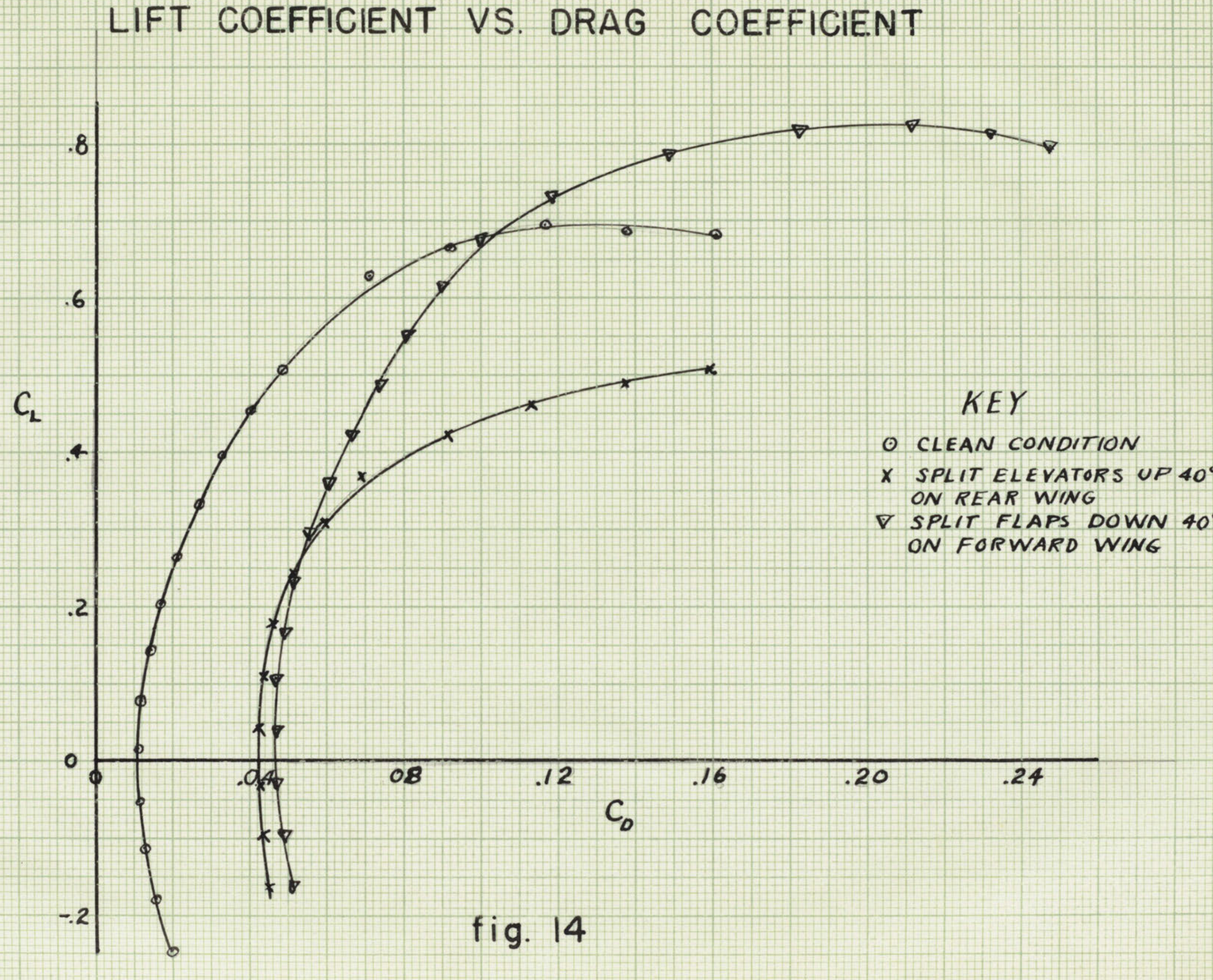
LIFT COEFFICIENT VS. DRAG COEFFICIENT
.8
.6
.4
.2
0
-.2
C_L
0
.04
.08
.12
.16
.20
.24
C_D
KEY
O CLEAN CONDITION
X SPLIT ELEVATORS UP 40° ON REAR WING
▽ SPLIT FLAPS DOWN 40° ON FORWARD WING

fig. 14

LIFT - DRAG POLAR

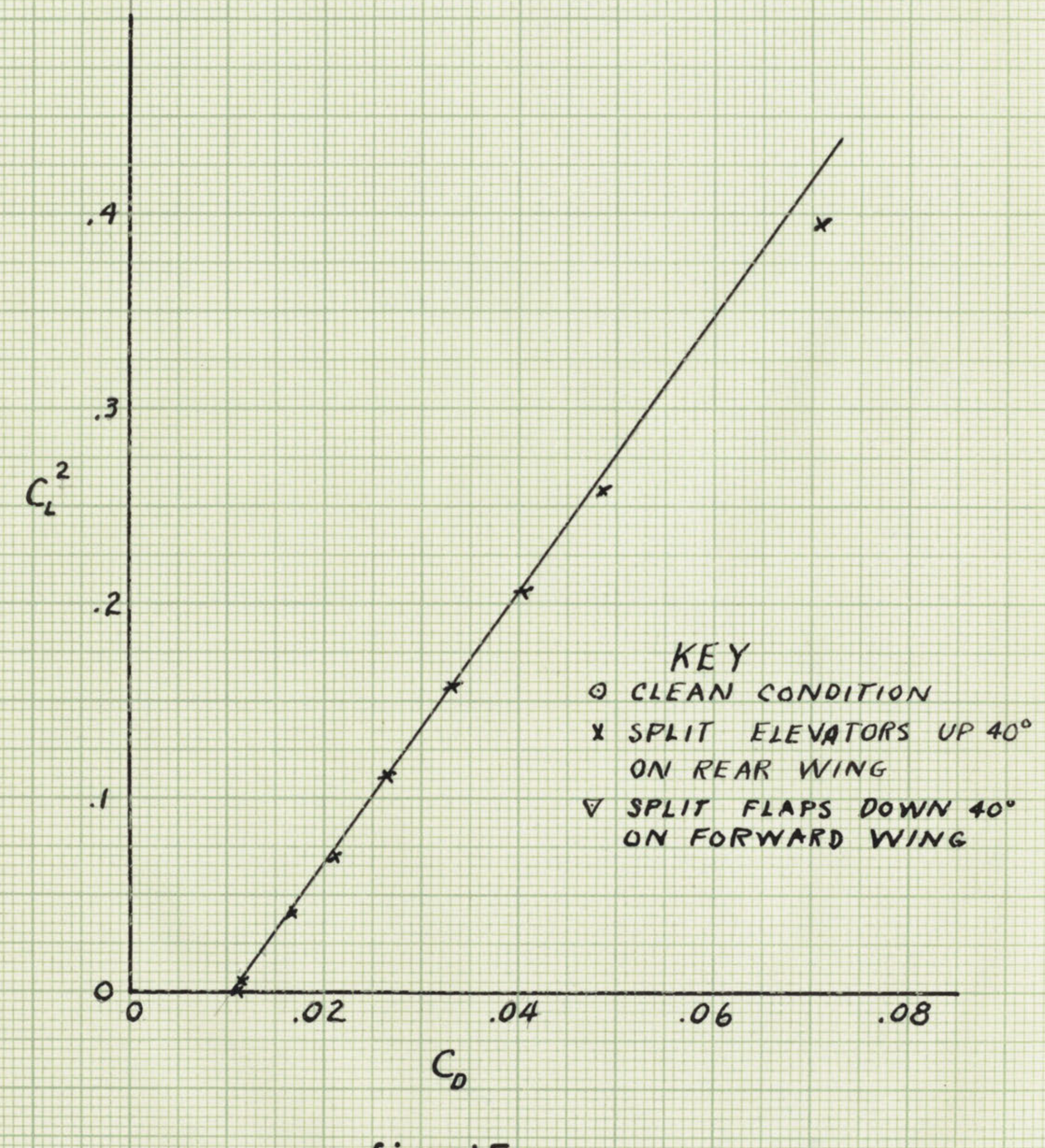

fig. 15

APPENDIX

TABLE I
VALUES OF F FUNCTION

Lift Stations

D.W. PTS.	1	2	3	4	5	6
1	4.24	-1.25	- .233	- .066	- .0521	- .030
2	- .99-	4.24	-1.25	- .233	- .096	- .048
3	- .12	- .99	4.24	-1.25	- .233	- .084
4	- .043	- .12	- .99	4.24	- .125	- .190
5	- .0220	- .043	- .12	- .99	4.24	- .99
6	- .017	- .030	- .064	- .190	-1.25	4.24
7	- .0135	- .0220	- .039	- .084	- .233	-1.25
8	- .0108	- .0162	- .0264	- .048	-.096	- .233
9	- .0089	- .0125	- .0186	- .030	- .0521	- .096
10	.8429	.0930	- .0968	- .0677	- .0436	- .0273
11	.0930	.8266	.0797	- .1043	- .0718	- .0436
12	- .0968	.0797	.8145	.0726	- .1085	- .0718
13	- .0677	- .1043	.0726	.8089	.0689	- .1085
14	- .0436	- .0718	- .1085	.0689	.8062	.0689
15	- .0273	- .0436	- .0718	- .1085	.0689	.8089
16	- .0180	- .0273	- .0436	- .0718	- .1085	.0726
17	- .0124	- .0180	- .0273	- .0436	- .0718	- .1043
18	- .0089	- .0124	- .0180	- .0273	- .0436	- .0677

TABLE I (cont'd)
VALUES OF F FUNCTION

Lift Stations

D.W. PTS.	7	8	9	10	11	12
1	- .0186	- .0125	- .0089	.6904	.0094	- .1870
2	- .0264	- .0162	- .0108	.0094	.0097	- .0438
3	- .039	- .0220	- .0135	- .1870	- .0438	- .0381
4	- .064	- .030	- .017	- .1347	- .2046	- .0267
5	- .12	- .043	- .0220	- .0890	- .1439	- .2162
6	- .99	- .12	- .043	- .0580	- .0890	- .1439
7	4.24	- .99	- .12	- .0402	- .0580	- .0890
8	-1.25	4.24	- .99	- .0281	- .0402	- .0580
9	- .233	-1.25	4.24	- .0078	- .0281	- .0402
10	- .0180	- .0124	- .0089	4.24	- .99	- .12
11	- .0273	- .0180	- .0124	-1.25	4.24	- .99
12	- .0436	- .0273	- .0180	- .233	-1.25	4.24
13	- .0718	- .0436	- .0273	- .096	- .233	-1.251
14	- .1085	- .0718	- .0436	- .0521	- .096	- .233
15	.0726	- .1043	- .0677	- .030	- .047	- .084
16	.8145	.0797	- .0968	- .0186	- .0264	- .039
17	.0797	.8266	.0930	- .0125	- .0162	- .0220
18	- .0968	.0930	.8429	- .0089	- .0108	- .0135

TABLE I(cont'd)
VALUES OF F FUNCTION

Lift Stations

D.W PTS.	13	14	15	16	17	18
1	- .1347	- .0890	- .0580	- .0402	- .0281	- .0078
2	- .2046	- .1439	- .0890	- .0580	- .0402	- .0281
3	- .0267	- 2.62	- .1439	- .0890	- .0580	- .0402
4	- .0213	- .0158	- .2162	- .1439	- .0890	- .0580
5	- .0158	- .0082	- .0158	- .2161	- .1439	- .0890
6	- .2162	- .0158	- .0213	- .0267	- .2046	- .1347
7	- .1439	- .2162	- .0267	- .0381	- .0438	- .1870
8	- .0890	- .1439	- .2046	- .0438	.0097	.0094
9	- .0580	- .0890	- .1347	- .1870	.0094	.6904
10	- .043	- .021	- .017	- .0135	- .0108	- .0089
11	- .12	- .043	- .030	- .0220	- .0162	- .0125
12	- .99	- .12	- .064	- .039	- .0264	- .0186
13	4.24	- .99	.190	- .084	- .047	- .030
14	-1.25	4.24	-1.25	- .233	- .096	- .0521
15	- .190	- .99	4.24	-1.25	- .233	- .096
16	- .064	- .12	- .99	4.24	-1.25	- .233
17	- .030	- .043	- .12	- .99	4.24	- 1.25
18	- .017	- .021	- .043	- .12	- .99	4.24

TABLE II
COEFFICIENTS OF CIRCULATIONS FOR THEORETICAL

CALCULATIONS OF SPANWISE LOAD DISTRIBUTION

D.W. PT.	K_1	K_2	K_3	K_4	K_5
1	4.231	-1.263	-..2516	- .126	- .0521
2	-1.0008	4.228	-1.276	- .281	- .096
3	- .1335	-1.012	4.201	-1.334	- .233
4	- .060	- .150	-1.054	4.05	- .125
5	- .0440	- .086	- .240	-1.98	4.24
10	.8340	.0806	- .1148	- .0950	- .0436
11	- .0806	.8086	.0524	- .1479	- .0718
12	- .1148	.0524	.7709	.0008	- .1085
13	- .0950	- .1479	.0008	.7004	.0689
14	- .0872	- .1436	- .2170	.1378	.8062
15					

TABLE II (cont'd)
COEFFICIENTS OF CIRCULATIONS FOR THEORETICAL

CALCULATIONS OF SPANWISE LOAD DISTRIBUTION

D.W. PT	K_{10}	K_{11}	K_{12}	K_{13}	K_{14}
1	.6826	- .0187	- .2272	- .1927	- .0890
2	- .0187	- .0305	- .1018	- .2936	- .1439
3	- .2272	- .1018	- .1271	- .1706	- .2162
4	- .1927	- .2936	- .1706	- .2375	- .0158
5	- .1780	- .2878	- .4324	- .0316	- .0082
10	4.231	-1.008	- .1335	- .060	- .021
11	- 1.263	4.224	-1.012	- .150	- .043
12	- .2516	-1.276	4.201	-1.054	- .12
13	- .126	- .281	- .1334	4.05	- .99
14	- .1042	- .192	- .466	-2.50	4.24

TABLE III

COEFFICIENTS OF CIRCULATIONS
$\Gamma_1, \Gamma_2, \ldots, \Gamma_5$
FOR SOLUTION OF EQUATION 2.14

K_1	K_3	K_5	K_7	K_9
0.45813421	.98980111	0.69025124	- .18892406	- .90945395
.74535966	.57970789	- .087419630	- .38542295	.95985426
.89578935	- .18789561	- .66848184	.99659435	- .53715240
.97499445	- .78239081	.43523110	- .00209439	- .43145605
1.00000	-1.00000	1.00000	-1.00000	1.00000